Journal of Applied Electrochemistry **29**: 1241–1244, 1999.

Short communication

Voltammetric study of Al–Zn–Mg alloys in chloride solutions

J.A. GARRIDO[1], P.L. CABOT[1]*, R.M. RODRIGUEZ[1], E. PEREZ, A.H. MOREIRA[2], P.T.A. SUMODJO[3] and A.V. BENEDETTI[4]

[1]*Laboratori de Ciència i Tecnologia Electroquímica de Materials, Department de Química Física, UB, Martí i Franquès, 1, 08028 Barcelona, Spain*

[2]*Departamento de Química Analítica e Físico-Química, UFC, Campus do Pici, Bloco 940, 60-451-970, Fortaleza, CE, Brazil*

[3]*Instituto de Química, Cidade Universitaria, USP, CP 20780, CEP 01498, São Paulo, Brazil*

[4]*Departamento de Físico-Química, Instituto de Química, UNESP, CP 355, CEP 14800, Araraquara, SP, Brazil*

*(*author for correspondence, e-mail: p.cabot@dept.qf.ub.es)*

Received 6 October 1998; accepted in revised form 13 April 1999

Key words: alloys, Al–Zn–Mg, chloride solutions

1. Introduction

Al–Zn–Mg alloys are age-hardenable materials which find many applications in aerospace and other transport areas [1]. High-strength, weldable and corrosion resistant Al–5%Zn–1.7%Mg alloys containing 0.2% Cu and sometimes with Cr and/or Nb, submitted to different heat treatments, were previously studied using cyclic voltammetry, open circuit potential measurements, metallography, SEM, TEM, EDX and XPS [2–5]. The cyclic voltammograms were obtained for low sweep rates, typically between 0.02 and 1 mV s^{-1}, in order to study the localized corrosion behaviour of these alloys [3, 5].

Chromium and niobium are not the most common alloying elements in Al–Zn–Mg alloys. However, the use of 0.15–0.25% Cr can be recommended for stress corrosion cracking (SCC) resistant, high-strength and weldable Al–(4.90–5.2%)Zn–(1.6–1.8%)Mg alloys [2, 4, 5]. The use of Nb has recently been considered [4–6], the results showing an increase in the fatigue resistance of the alloy, the effect of a slight reduction of its grain size and also a small increase in the pitting corrosion resistance.

Specimens submitted to interrupted quenching and artificial ageing presented cyclic voltammograms with an anodic maximum before the pit propagation region [3, 5]. SEM observations showed that no pitting took place in the region of the anodic maxima, but a surface transformation involving all the alloy surface (rough oxidized film was present). The anodic peak disappeared after the first cycle when the cyclic voltammetry was performed between the passive region and after the current decay following the anodic peak. The anodic charge corresponding to such maxima increased only slightly with sweep rate in the sweep rate range studied and decreased in the presence of small amounts of Cr and Nb. In addition, no effect of stirring on these anodic charges was found, thus indicating that such anodic maxima were not related to diffusion control in the electrolyte. These results and XPS analyses showed that such anodic maxima corresponded to Mg depletion at the oxide/alloy interface, together with some oxide growth and dissolution. Magnesium was probably transported through the oxide film defects, these defects being produced by the chloride penetration. To the authors knowledge, no similar characteristics have been described in the literature on Al–Zn–Mg alloys. These alloys were SCC resistant, in agreement with breaking stress experiments [7], because, according to the theory of Galvele and de Micheli [8] and to the results of Maitra and English [9], these maxima did not correspond to intergranular pitting attack.

As stated above, cyclic voltammetry at low sweep rates was applied previously to study the resistance to localized corrosion of the present Al–Zn–Mg alloys. In this work, linear sweep voltammetry over a wide range of sweep rates has been applied to study the kinetics of the processes related to these anodic maxima and thus, to obtain further insight into the reaction mechanism. The results have been interpreted on the light of theoretical models and previous work.

2. Experimental details

The alloys studied were H, J, L and O, and their compositions are given in Table 1. Alloy cylinders 3 mm in diameter were submitted to heat treatment B (quenched, naturally aged for three days at 25 °C and then, artificially aged for 8 h at 90 °C, and for 24 h at 135 °C) or to heat treatment C (quenched, interrupted for 2 min at 400 °C, and aged as B) [3–5]. Afterwards, they were embedded in epoxy resin and polished using

Table 1. Compositions of the Al–Zn–Mg alloys under study (in wt % by spectrophotometric analysis) with Fe, Ni, V and Mn contents less than 0.001%

Alloy	Zn	Mg	Cu	Cr	Nb	Si	Ti
H	5.0	1.7	0.23	< 0.001	< 0.01	0.006	< 0.001
J	5.0	1.7	0.23	< 0.001	0.053	0.006	< 0.001
L	5.0	1.7	0.24	0.140	< 0.01	0.007	< 0.001
O	5.0	1.6	0.24	0.140	0.053	0.001	0.003

diamond paste up to 1 μm finish and cleaned with ethanol in an ultrasonic bath. Only one base of the alloy cylinder was exposed to the electrolyte.

The electrochemical cell, alloys and instrumentation were the same as those reported elsewhere [5]. The experiments were performed in a three-electrode cell at 25.0 ± 0.1 °C. A SCE and a Pt mesh were used as reference and auxiliary electrodes, respectively (all the potentials given are referred to the SCE). The working electrolyte was 0.5 mol dm^{-3} NaCl (Merck p.a.), prepared with distilled water filtered through a Millipore Milli-Q system. The voltammetric experiments were performed in quiescent and deaerated electrolyte using a PAR 273 potentiostat and the 342C PARC corrosion software. The initial potentials in the voltammetric experiments were −1.2 V, which was about the open circuit potential in deaerated NaCl solutions [4, 5], and sweep rates in the range 0.02–80 mV s^{-1} were applied.

3. Results and discussion

The voltammograms obtained at different sweep rates for the specimens H, J, L and O submitted to heat treatments B and C are exemplified in Figures 1 and 2. The shape of the voltammograms were the same independently of the presence of Cr and Nb. Curves of this type, for low sweep rates, were interpreted elsewhere [5]. As shown in Figure 1, for all the

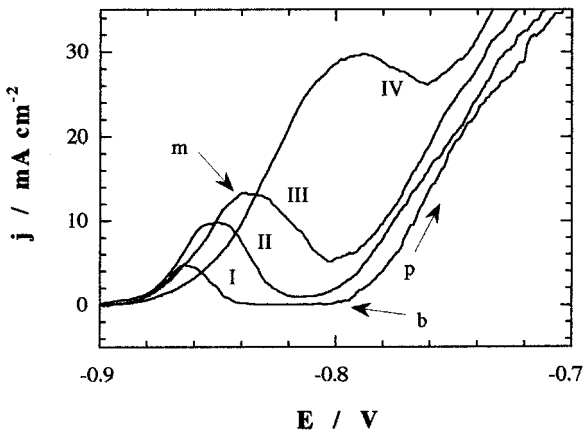

Fig. 1. Voltammograms obtained for alloy HC in deaerated and quiescent 0.5 mol dm^{-3} NaCl at different sweep rates: (I) 0.6, (II) 1.2, (III) 2 and (IV) 5 mV s^{-1}.

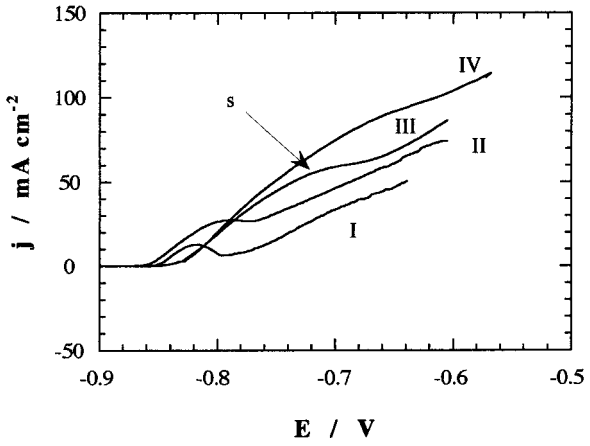

Fig. 2. Voltammograms obtained for alloy OB in deaerated and quiescent 0.5 mol dm^{-3} NaCl at different sweep rates: (I) 2, (II) 5, (III) 30 and (IV) 80 mV s^{-1}.

specimens studied, a passive region is found during the initial stages of the anodic sweep and afterwards, an anodic peak (m) appears. This peak was related to the alloy oxidation involving all the alloy surface together with a Mg depletion at the alloy/oxide interphase (surface dealloying with transport of Mg cations through the film defects to the solution). Some oxide formation and dissolution was also demonstrated by XPS and then, some kind of passivation takes place. The current goes to zero after the anodic maximum for the lowest sweep rates applied, but this does not preclude the alloy pitting found for more positive potentials. Small anodic maxima before pitting were also previously observed in Al–Fe alloys [10]. In this case, the anodic maxima were related to iron oxidation on the iron intermetallic compounds. After this anodic peak, the current increases due to film breakdown (b) and pit propagation (p).

In the low sweep rate range, that is from 0.02 to 1–2 mV s^{-1}, these peaks are completely separated from the pitting corrosion region. However, when the sweep rate increases, both the anodic peak and the breakdown potential are shifted to more positive potentials with a resultant increasing overlap, shown in Figure 2. For high sweep rates, these peaks appear as a shoulder(s) in a net current increase. The separation between the anodic peak and the breakdown potential was slightly higher for alloys H and J than for alloys L and O.

The peak current (j_m) and peak potential (E_m) plots against the square root of the sweep rate, $v^{1/2}$, for different specimens, to test whether the kinetics of the anodic maxima follow a mass transfer control [11–13], have been plotted in Figures 3 and 4. The peak current densities measured for the highest sweep rates differed about 5 mA cm^{-2} for all the specimens studied (Figures 3(a) and 4(a)), but no sequence in the peak currents could be found. In contrast, significant differences in the peak potentials appeared for the two groups of alloys, that is those containing chromium (L and O, heat treatments B and C) and those which did not contain

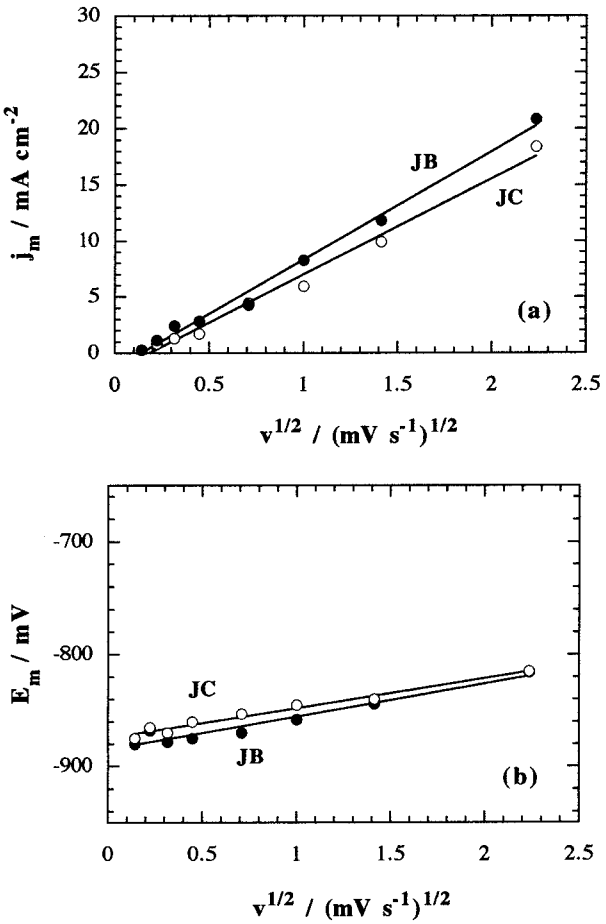

Fig. 3. Peak current, j_m (a), and peak potential, E_m (b), against the square root of sweep rate, $v^{1/2}$, for the specimens JB and JC.

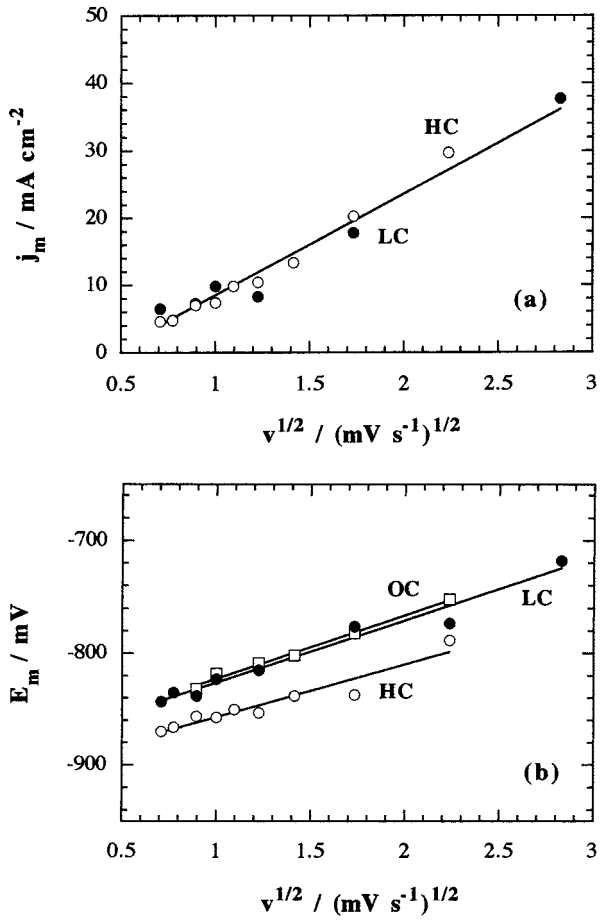

Fig. 4. Peak current, j_m (a), and peak potential, E_m (b), against the square root of sweep rate, $v^{1/2}$, for the specimens indicated.

chromium (H and J, heat treatments B and C). This is exemplified in Figure 4(b). The peak potentials corresponding to the specimens H and J were more negative than those found for the specimens L and O. This appears to be related to the significant increase in the pitting corrosion resistance produced by the presence of Cr in the aluminium alloys [4, 5, 14, 15]. The anodic peak potentials, and the breakdown and repassivation potentials, were all shifted in the positive direction. The shift of the breakdown and repassivation potentials was related to an increase in the pitting corrosion resistance [4, 5, 14, 15], and this was explained by the presence of Cr in the anodic film, which restricted the chloride from reaching the metal/film interface. The increase in the pitting corrosion resistance with Cr and Nb is not then due to a surface depletion of Mg, but to the presence of these elements in the oxide layer. This also explains the shift of the anodic maxima to more positive potentials with Cr because the Mg depletion was related to the ingress of chloride into the anodic film [5], and Cr in the film could restrict the chloride penetration to more positive values. In addition, it could limit the Mg depletion and the oxide dissolution by chloride, because the charges of such anodic maxima were lower when the alloy contained Cr [5]. Chromium and niobium did not influence the shape of the voltammograms but limited the chloride attack.

Despite good linearity being obtained in the j_m and E_m against $v^{1/2}$ plots, to establish the relationship between j_m and v, double logarithmic plots were also made. The power of v in the j_m against v^x equation can be obtained from the slope of the log j_m against log v plots. From these plots, values of x of 0.7 ± 0.1 were obtained for all the specimens studied. Thus, the processes related to these anodic maxima do not appear to fit to a simple model.

Linear j_m against $v^{1/2}$ and E_m against $v^{1/2}$ plots have been predicted in the case of growth of new phases on metal surfaces both under diffusion control (of species in solution or in the film on the metal) [11, 12], and also under migration control (of species through a porous film) [12, 13]. However, migration control with growth of a passivating film according to Müller's model is discarded in our case, taking into account that aluminium and aluminium alloys always appear to be covered by a passivating oxide film in the pH range 3 to 9 [16], the amorphous nature of this oxide [16] and the surface transformation reported elsewhere [5]. Proportionalities between I_m and $v^{0.5}$ or $v^{0.6}$ have also been described for nucleation and growth of crystals [17]. However, no evidence of crystal growth processes after the anodic

maxima were found for the specimens studied here [5]. Stirring did not change the charges of the anodic maxima [5] and therefore we have to think in terms of solid state phase formation/transformation as a result of a dealloying process.

The present results, together with those previously reported, suggest that the processes corresponding to the anodic maxima found in the voltammograms shown in Figures 1 and 2 are, at least partially, controlled by mass transport through the defective film which is being formed on the alloy. The situation resembles other cases described in the literature for other systems such as copper [18–20], in which a proportionality between I_m and $v^{0.8}$ was obtained for the Cu(II) peak in alkaline solutions, this result being interpreted assuming a mixed control by diffusion and surface steps. There are several possibilities in the case of the present alloys, because solution phase diffusion, diffusion through pores and surface and solid state diffusion may take place. However, solution phase diffusion is not considered to be relevant because no effect of stirring in the peak charge was found [5]. On the other hand, the peak current against sweep rate analysis could only be performed for sweep rates in the range 0.1–10 mV s^{-1} because of peak overlap with pit propagation. Although the extension to much higher sweep rates would be interesting in the definition of the current against sweep rate behaviour, the present analysis had to be restricted to sweep rates lower than 10 mV s^{-1}. Similar sweep rate ranges were also employed in other work for model testing [19, 20]. It has to be taken into account, however, that a mass transport process through the surface film is being suggested in our case, and probably, high sweep rates are not necessary to show mass transport control. In addition, some oxide film growth was shown to coexist with such anodic maxima [5]. This explains the deviation from 1/2 in the slope of the double logarithmic j_m against v plots discussed above. A similar interpretation was suggested by Hampson et al. [20] for copper in alkaline solutions, in which the rate determining step appeared to be the transport of the oxidation product by diffusion from the surface to the solution. The deviation from 1/2 in the slope of such double logarithmic plots for sweep rates greater than 25 mV s^{-1} was explained by the production of Cu(II) oxide, which hampered the current flow. Further constant potential experiments are being performed to obtain deeper insight into the kinetics of this particular process affecting the present Al–Zn–Mg alloys.

Acknowledgements

The authors gratefully acknowledge the financial support of this work by the DGICYT (Spain), project PB91-0260 and the grant conceded to A.H. Moreira by the CNPq (Brazil).

References

1. 'Corrosion', *in* 'Metals Handbook', 9th edn, Vol. 13, (ASM, Metals Park, OH, 1987), pp. 583–609.
2. H. Cordier, C. Dumont, W. Gruhl and B. Grzemba, *Metall.* **36** (1982) 33.
3. P.L. Cabot, F. Centellas, J.A. Garrido, R.M. Rodríguez, E. Brillas, E. Pérez, A.V. Benedetti and P.T.A. Sumodjo, *J. Appl. Electrochem.* **22** (1992) 541.
4. P.L. Cabot, J.A. Garrido, E. Pérez, A.H. Moreira, P.T.A. Sumodjo and A.V. Benedetti, *J. Appl. Electrochem.* **25** (1995) 781.
5. J.A. Garrido, P.L. Cabot, A.H. Moreira, R.M. Rodrícguez, P.T.A. Sumodjo and E. Pérez, *Electrochim. Acta* **41** (1996) 1933.
6. M. Cilense, PhD. thesis, Araraquara, Brazil (1990).
7. W. Gárlipp, S. Saimoto and H.M. dos Santos, *Proceedings of the Meeting of the Associaçao Brasileira de Metais*, Belo Horizonte, M.G., Brazil (1987), pp. 33–44.
8. J.R. Galvele and S.M. de Micheli, *Corros. Sci.* **10** (1970) 795.
9. S. Maitra and G.C. English, *Metall. Trans.* **12A** (1981) 535.
10. O. Seri and K. Tagashira, *Corros. Sci.* **30** (1990) 87.
11. S. Fletcher, C.S. Halliday, D. Gates, M. Westcott, T. Lwin and G. Nelson, *J. Electroanal. Chem.* **159** (1983) 267.
12. M. Noel and K.I. Vasu, *in* 'Cyclic Voltammetry and the Frontiers of Electrochemistry', (Aspect Publications Ltd, London, 1990), pp. 370–406.
13. D.D. Macdonald, *in* 'Transient Techniques in Electrochemistry', (Plenum, New York, 1977), chapter 8.
14. W.C. Moshier, G.D. Davis and G.O. Cote, *J. Electrochem. Soc.* **136** (1989) 356.
15. G.D. Davis, W.C. Moshier, T.L. Fritz and G.O. Cote, *J. Electrochem. Soc.* **137** (1990) 422.
16. P.A. Malachesky, *in* A.J. Bard, 'Encyclopedia of Electrochemistry of the Elements' Vol. VI (Dekker, New York, 1976), chapter 3, p. 103.
17. S. Fletcher, *J. Electroanal. Chem.* **118** (1981) 419.
18. S.L. Marchiano, C.I. Elsner and A.J. Arvía, *J. Appl. Electrochem.* **10** (1980) 365.
19. A.V. Benedetti, R.Z. Nakazato, P.T.A. Sumodjo, P.L. Cabot, F. Centellas and J.A. Garrido, *Electrochim. Acta* **36** (1991) 1409.
20. N.A. Hampson, J.B. Lee and K.I. Macdonald, *J. Electroanal. Chem.* **32** (1971) 165.